








## Research Article

# Grass pollen surface ornamentation is diverse across the phylogeny: Evidence from northern South America and the global literature

Cai-Xia Wei<sup>1\*</sup> , Phillip E. Jardine<sup>2</sup> , Li-Mi Mao<sup>3</sup> , Luke Mander<sup>4</sup> , Mao Li<sup>5</sup> , William D. Gosling<sup>1</sup> , and Carina Hoorn<sup>1</sup> 

<sup>1</sup>Institute for Biodiversity and Ecosystem Dynamics, University of Amsterdam, Amsterdam, The Netherlands

<sup>2</sup>Institute of Geology and Palaeontology, University of Münster, Münster, Germany

<sup>3</sup>The State Key Laboratory of Palaeobiology and Stratigraphy, Nanjing Institute of Geology and Palaeontology, Chinese Academy of Sciences, Nanjing, China

<sup>4</sup>Department of Environment, Earth and Ecosystems, The open University, Milton Keynes, UK

<sup>5</sup>Donald Danforth Plant Science Center, Saint Louis, MI, USA

\*Author for correspondence. Caixia Wei. E-mail: caixiawei1994@gmail.com

Received 24 March 2023; Accepted 21 August 2023

**Abstract** The grasses are one of the most diverse plant families on Earth. However, their classification and evolutionary history are obscured by their pollen stenopalynous (similar) morphology. A combination of high-resolution imaging of pollen surface ornamentation and computational analysis has previously been proposed as a promising tool to classify grass taxonomic boundaries. In this study, we test this hypothesis by studying Poaceae pollen across the phylogeny from plants collected in northern South America and also from published literature across the globe. We assessed if morphotypes that we establish using descriptive terminology are supported by computational analysis, if they vary along six (a)biotic variables and vary across the phylogeny. Based on this analysis, we constructed a reference framework for pollen surface ornamentation morphotypes. Our results showed that there is a wide variation of grass pollen surface ornamentation. We identified nine new and confirmed six known morphotypes, establishing a data set for 223 species (243 individual plant specimens) that represent 11 subfamilies. Computational analysis showed that our morphotypes are well-supported by two quantitative features of pollen sculptural elements (size and density). The specific data set and mapping of the phylogeny confirmed that pollen morphological sculpture is unrelated to (a)biotic variables and is diverse across the phylogeny.

**Key words:** computational analysis, exine, grass, phylogeny, pollen morphology, quantitative analysis.

## 1 Introduction

The grass family (Poaceae) originated in the Cretaceous (Prasad et al., 2005; Poinar et al., 2015; Wu et al., 2018; Gallaher et al., 2022) and diversified into 12 subfamilies, with approximately 11 783 species today (Linder, 1987; White et al., 2000; Stromberg, 2011; Soreng et al., 2022). Grasses occur on all continents, including Antarctica, ranging across different latitudes and ecosystem types (Gibson, 2009; Linder et al., 2018). Although Poaceae have a long (>100 Ma) vegetation history, there is a substantial knowledge gap regarding their evolutionary and ecological history due to the lack of available fossil data.

Pollen morphology has been regarded as an ideal method when studying the microbotanical fossil record

(e.g., Ferguson et al., 1977; Page, 1978; Beug, 2004; Mander et al., 2013), and can provide important information on taxonomic boundaries and classification. Nevertheless, it is difficult to classify fossil grass pollen in terms of extant genera or even subfamilies, as there is no complete Poaceae pollen reference data set of extant species. Moreover, Poaceae pollen is stenopalynous (principally monoporate and psilate) and, therefore, very similar within the family (Page, 1978; Salgado-Labouriau & Rinaldi, 1990; Bush, 2002; Beug, 2004; Halbritter et al., 2018), although there have been reports of grass pollen with two to three pores rather than the usual single pore (Mercuri et al., 2022). Recently Wei et al. (2023) showed that the pollen size of undomesticated grasses cannot easily be used to reconstruct past vegetation or climate

This is an open access article under the terms of the Creative Commons Attribution License, which permits use, distribution and reproduction in any medium, provided the original work is properly cited.

parameters. In addition, glycerin jelly, a commonly used mounting medium in palynological processing procedures, has been found to affect pollen size during pollen storage (Wei et al., 2023). This all means that it is challenging to reconstruct the history of grasses using simple characters that can be measured with transmitted light microscopy.

In spite of the stenopalynous of grass pollen morphology, since the 1970s, a high degree of variability in grass pollen surface ornamentation has been observed when using scanning electron microscopy (SEM) (e.g., Andersen & Bertelsen, 1972; Page, 1978; Köhler & Lange, 1979). Scientists have made several attempts to classify grass pollen based on this variability. Page (1978) tried to recognize exine patterns based on granules being fused or separated but found that they could not build a classification based on such features. Köhler & Lange (1979) first proposed that the pollen surface ornamentation can be classified into different morphotypes, such as *Hordeum*-type, *Triticum*-type, *Avena*-type, and *Setaria*-type. Subsequently, a new *Pariana*-type and *Stipa*-type were identified (Mander & Punyasena, 2015). Nevertheless, the commonness or rarity of each morphotype remained unclear due to the low number of documented specimens with a clear surface pattern. Analyzing pollen morphology under electron microscopy and superresolution microscopy with computational image analysis is now a developing tool that can resolve these problems (Mander et al., 2013; Romero et al., 2020).

Special ornamentation structures in grass pollen might be useful as an additional indicator to understand the fossil record. For instance, the “rugulate” shape and the “orbicular” ornamentation pattern are two morphological forms that have been previously documented (e.g., Vinckier & Smets, 2001; Dórea et al., 2017; Guimarães et al., 2018; Ruggiero & Bedini, 2018). The “rugulate” shape consists of elongated irregular ridges, whereas “orbicules” consist of distinctive granules (Punt et al., 2007). Souza et al. (2021) confirmed that the rugulate ornamentation of *Dendrocalamus asper* (Schult. & Schult. f.) Backer ex K. Heyne is only shown during pollen maturation, which is related to flowering inflorescence development. Furthermore, Lovisolo & Galati (2012) proposed that the occurrence of orbicules might be different in different subfamilies, and they defined orbicules in the subfamily Pooideae as spherical corpuscles with a spiculated surface, Chloridoideae as plate-like corpuscles, and Panicoideae as subspherical corpuscles, respectively. The orbicular ornamentation pattern is also relevant in the field of allergy studies. It was hypothesized that orbicules make grass pollen an important vector as an allergen (Vinckier & Smets, 2001). Therefore, exine structure could be a factor when attempting to understand allergies in relation to pollen.

In this study, we ask the following questions: (i) *Can pollen morphotypes help us to differentiate and classify Poaceae at different taxonomic levels?* (ii) *Can such classification be supported by quantitative morphometric data of surface ornamentation?* and (iii) *Does the pollen surface ornamentation vary in concert with key explanatory parameters, or systematically across the grass phylogeny?* To achieve this, we took SEM images on the pollen surface ornamentation for 803 pollen grains, which were collected from northern South America from 68 plant specimens belonging to 55 species

from nine subfamilies across the Poaceae phylogeny. We also reviewed the literature and identified additional morphotypes from published SEM images of grass pollen surface ornamentation from 170 species (175 specimens). Based on our SEM imagery data, we constructed a database of 15 surface ornamentation morphotypes in total (including five types from published literature). The database helped us assess how these morphotypes are distributed among the grass taxa. We also extracted the size and density of sculptural elements on the surface of grass pollen grains. We used image processing to test the degree to which the morphotypes in our database are supported by quantitative measurements of morphology. We also correlated grass pollen surface ornamentation with explanatory variables, and we mapped morphotype occurrence onto the grass phylogeny in order to explore how pollen sculpture ornamentation varies across the Poaceae phylogeny.

## 2 Material and Methods

### 2.1 Materials and methods for our samples

#### 2.1.1 Sample collection and processing

The pollen grains were sampled from 55 species of 68 plant specimens from the Naturalis Biodiversity Center of the Netherlands (NHN-L). These specimens were all deposited in the collection between 1808 and 2012 and were all collected from northern South America (Fig. 1). Two to three specimens from eight species belonging to six subfamilies were selected here for testing the variability within species, including *Aristida recurvata* Kunth, *Calamagrostis effusa* (Kunth) Steud., *Chusquea tessellata* Munro, *Echinochloa colona* (L.) Link, *Paspalum repens* P.J. Bergius, *Poa annua* L.,



**Fig. 1.** Study area and localities where the herbarium specimens were collected and which we used in this study. Symbol colors denote the Poaceae subfamily; the map was modified from Wei et al. (2023).

*Sporobolus indicus* (L.) R.Br., and *Streptochaeta spicata* Schrad. ex Nees. The specimen information (country and year, collector information, location, elevation, photosynthetic pathway, climate data, vegetation type, and soil type) can be found in Appendix S1.

All pollen samples were available through previous research and methods are reported in Wei et al., 2023). In the present study, we transferred the pollen from glycerin jelly to ethanol with a gradual concentration series (70%, 96%, and 100%), to remove the glycerin jelly and dehydrate the grains ahead of SEM imaging.

### 2.1.2 SEM image acquisition

Dehydrated pollen grains were transferred to SEM stubs and coated with Platinum gold, then scanned with SEM (TESCAN MAIA3, Czech) under 20 kV at the Nanjing Institute of Geology and Palaeontology, Chinese Academy of Sciences (NIGPAS). At least, nine pollen grains were examined and imaged for each plant specimen. Each pollen grain was imaged under three amplification levels:  $\times 15\,000$ ,  $\times 75\,000$ , and  $\times 150\,000$ . All images were saved in high resolution for morphological analysis.

### 2.1.3 Palynological morphotype description of Poaceae

The pollen surface ornamentation was described based on the SEM images and each specimen was grouped into one specific morphotype. The descriptions of new morphotypes follow Punt et al. (2007). Six established known morphotypes refer to previous work (Köhler & Lange, 1979; Mander & Punyasena, 2015).

### 2.1.4 Quantifying pollen surface ornamentation with size and density of sculptural elements

Quantitative analysis was undertaken on  $3.3\ \mu\text{m}^2$  ( $1855 \times 1855$  pixel) windows that were manually cropped from the  $\times 150\,000$  images (Figs. 2A1, 2B1). Size and density were extracted from the pollen surface ornamentation of each

SEM image using the method adapted from the approach developed by Mander et al. (2013). First, contrast-limited adaptive bell-shaped histogram equalization was used for adjusting the image contrast (Figs. 2A2, 2B2). Subsequently, five subimages with  $1000 \times 1000$  pixels were randomly chosen and cropped from each  $1855 \times 1855$  image. For each subimage, Sobel approximation was applied to detect edges with maximum gradient, then morphological closing (a dilation process followed by an erosion process) was performed to connect scatter points (Figs. 2A3, 2B3). We then identified the first 10 largest connected components. For each connected component, we performed principal component analysis (PCA) and calculated the value of PC1 projection as its size. We took the average size for the first 10 largest connected components as the size of each subimage (Figs. 2A4, 2B4). Finally, we took the average of the size features for the five subimages as the first feature [size] of one  $1855 \times 1855$  image.

Afterwards, each subimage was quantized into four colors by minimum variance quantization and the brightest color was used as the foreground (i.e., binarize the image, Figs. 2A5, 2B5). We then performed morphological closing on the binary image to connect the scatter points and counted the connected components with the areas larger than a threshold as the density of the subimage. We then took the average of all density features for the five subimages; the second feature [density] was obtained (Figs. 2A6, 2B6).

The value of size and density feature of each grain of northern South American samples are provided in Appendix S2.

### 2.1.5 Data and software

**2.1.5.1 Data collection.** Here, we compiled existing research on the C3/C4 photosynthetic pathway, which includes 12 153 grass species in total (Appendix S3). Photosynthetic pathways assigned to each species came from previous research and references therein (Renvoize, 1981, 1986; Wills et al., 2000;

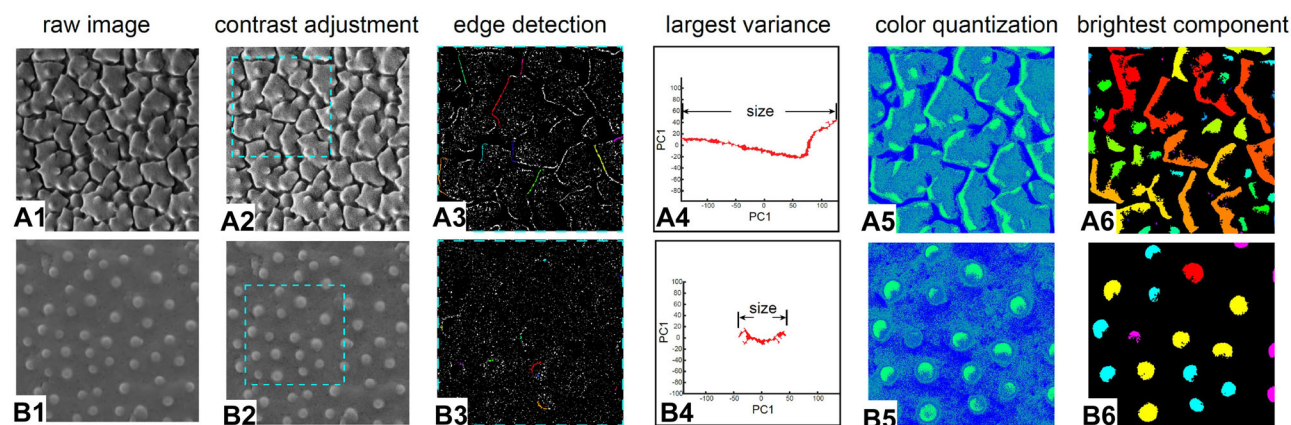


**Fig. 2.** Thumbnails showing the example of image processing steps that were taken during the construction of features size and density. **A1–A6**, *Poa horridula* Pilg. **B1–B6**, *Tristachya leiostachya* Nees. (A1–B1) shows raw images ( $1855 \times 1855$  pixels) with different morphotypes. (A2–B2) shows adjusting the image contrast and an example of randomly cropping subimages with  $1000 \times 1000$  pixels. (A3–B3) shows the Sobel edge detection for each subimage. (A4–B4) shows the size feature for one of the connected components, with 1807 and 155 for *P. horridula* and *T. leiostachya*, respectively. (A5–B5) shows the four colors quantized for each subimage. (A6–B6) shows connected components using the brightest color as the foreground, which is used for counting the density feature for each subimage, with 60 and 21 for *P. horridula* and *T. leiostachya*, respectively.

Ibrahim et al., 2009; Christin et al., 2013; Osborne et al., 2014; Kadereit et al., 2017; Moore et al., 2019; Gallaher et al., 2022; Soreng et al., 2022).

The vegetation type, soil type, elevation, mean annual temperature (MAT), and total annual precipitation (TAP) data for each of our northern South America samples were taken from Wei et al. (2023).

**2.1.5.2 Data visual exploration.** The size and density values from the image processing step were transferred to log size and log density before being used in data analyses, which aimed to make the data closer to a normal distribution. Box plots, scatter plots, and linear regression were used to explore and visualize the data.

**2.1.5.3 Software, SEM images, and data availability.** All image processing and feature extraction were carried out in MATLAB (R2017a). All data analysis and visualization were carried out using R v.4.1.1 (R Core Team, 2021). All original SEM images of grass pollen ornamentation for extracting quantitative features, the MATLAB code for quantitative analysis, and the R code for data analysis are available for download from figshare: <https://doi.org/10.6084/m9.figshare.23302022.v3>

## 2.2 SEM images collection from literature and morphotypes assignment

We investigated SEM images from the literature for grass pollen surface ornamentation and each specimen was identified into one specific morphotype. For the morphotype identification, we referred to the work by Mander & Punyasena (2015), and also carried out an additional

search of the literature, with a main focus on work published after 2015 (Chaturvedi et al., 1998; Lee et al., 2004; López-Merino et al., 2015; Morgado et al., 2015; Needham et al., 2015; Dórea et al., 2017, 2018; Guimarães et al., 2018; Ruggiero & Bedini, 2018; Noor & Ahmad, 2021; Souza et al., 2021; Ullah et al., 2021; Visez et al., 2021; Anar et al., 2022; Toledo et al., 2022), and SEM figures of two species of *Oryza* provided by one of us (Limi Mao) (Appendix S4). The descriptions of new morphotypes from the literature follow Punt et al. (2007). In total, we assessed the pollen surface ornamentation of 223 species in 11 subfamilies, which represents 1.9% of 11783 grass species (Soreng et al., 2022).

## 3 Results

### 3.1 Poaceae pollen morphotypes

#### 3.1.1 Our samples

Based on our study of surface pollen ornamentation of 68 grass specimens, we assigned these specimens to 10 morphotypes (Appendix S1). Four of these 10 types are new morphotypes, including *Arthrostylidium*-type, *Muhlenbergia*-type, *Poa*-type, and *Streptochaeta*-type (Fig. 3A; Table 1). All six known morphotypes that were described in the earlier literature (Köhler & Lange, 1979; Mander & Punyasena, 2015) were found in our samples (Fig. 3B; Table 1). The descriptions of all morphotypes are provided in Appendix S5.

#### 3.1.2 Literature study

Through a literature search, we identified 175 specimens from 170 species belonging to 11 subfamilies present in clear

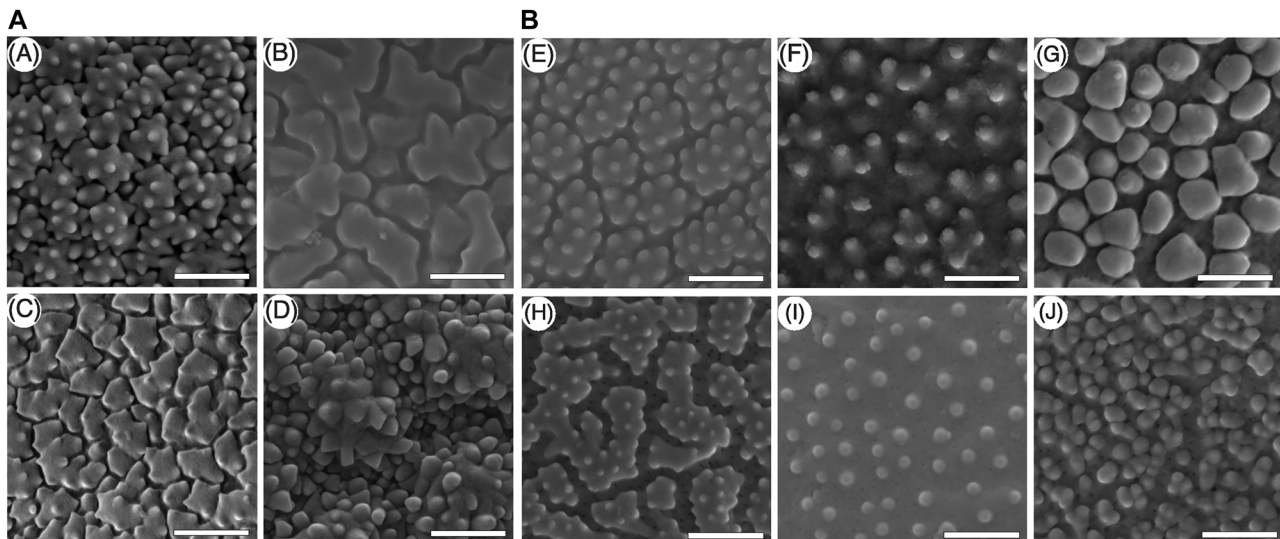


**Fig. 3.** **A**, Thumbnails showing examples of new morphotypes: (A) the *Arthrostylidium*-type, (B) the *Muhlenbergia*-type, (C) the *Poa*-type, (D) the *Streptochaeta*-type. Specimen shown in these thumbnails are as follows: (A) *Arthrostylidium subpectinatum* Kuntze (7707), (B) *Muhlenbergia ligularis* (Hack.) Hitchc. (7789), (C) *Poa horridula* (9055), (D) *Streptochaeta spicata* (9403). Scale bar = 1 µm. **B**, Thumbnails showing examples of known morphotypes: (E) the *Avena*-type, (F) the *Hordeum*-type, (G) the *Pariana*-type, (H) the *Setaria*-type, (I) the *Stipa*-type, (J) the *Triticum*-type. Specimens shown in these thumbnails are as follows: (E) *Bothriochloa pertusa* (9427), (F) *Festuca bromoides* L. (7879), (G) *Acicahne acicularis* Lægaard (7726), (H) *Arthrostylidium ecuadorensis* Judz. & L.G. Clark (7705), (I) *Tristachya leiostachya* (8665), (J) *Pharus latifolius* L. (9390). Scale bar = 1 µm.

**Table 1** The description of 10 grass pollen surface morphotypes from our samples.

Morphotypes	Overall	Areolae	Spinules/scabrate	Reticulum	Figures
<i>Arthrostylidium</i> -type	Areolae studded with 1–10 spinules	Larger irregular polygonal or elongated areolae	1–10	-	Fig. 3A-(A)
<i>Muhlenbergia</i> -type	Smooth areolae studded with very rarely spinules; narrow negative reticulum	Larger irregular polygonal or elongated outlines	Very rarely or none	Narrow grooves	Fig. 3A-(B)
<i>Poa</i> -type	Sharp areolae, studded with 1–10 spinules, narrow negative reticulum	Sharp angular areolae of irregular polygonal outlines	1–10, rarely more	Very narrow grooves	Fig. 3A-(C)
<i>Streptochaeta</i> -type	Rugulate ornamentation with dense single detached spinules	-	Dense single detached spinules with a different direction	-	Fig. 3A-(D)
<i>Avena</i> -type	Areolae studded with several 1–10 spinules; shallow negative reticulum	Medium to large, irregular polygonal or elongated areolae	1–10 spinules	Shallow grooves	Fig. 3B-(E)
<i>Hordeum</i> -type	Single detached spinule	Generally, not present	Dingle, detached spinules	-	Fig. 3B-(F)
<i>Pariana</i> -type	Spinulose areolate; deep negative reticulum	Globular/granular, smooth areolae, 0.2–0.8 $\mu\text{m}$ in diameter	Very rarely	Deep grooves	Fig. 3B-(G)
<i>Setaria</i> -type	“Field-like” areolae studded with small pointed spinules	“Field-like” areolae with irregular polygonal outlines	Very small pointed spinules, 1–10	Deep grooves	Fig. 3B-(H)
<i>Stipa</i> -type	Single granules; scabrate evenly distributed	-	Single, evenly dispersed granules; sparsely scabrate	-	Fig. 3B-(I)
<i>Triticum</i> -type	Small areolae studded by one to three spinules	Small areolae	1–3 spinules	Shallow grooves	Fig. 3B-(J)

Note that *Arthrostylidium*-type, *Muhlenbergia*-type, *Poa*-type, and *Streptochaeta*-type are new morphotypes, and their scanning electron microscope (SEM) images can be found in Fig. 3A. *Avena*-type, *Hordeum*-type, *Pariana*-type, *Setaria*-type, and *Triticum*-type are known morphotypes, and their SEM images can be found in Fig. 3B.

SEM images of grass pollen surface ornamentation. We identified 15 morphotypes in total (Appendix S7), and among them, the *Avena*-type, *Stipa*-type, *Hordeum*-type, and *Setaria*-type are the most common. Five of these 15 types were identified as new morphotypes, including *Anomochloa*-type, *Diandrolyra*-type, *Olyra juruana*-type, *Olyra bahiensis*-type, and *Sucrea*-type (Table 2). The descriptions of these five new morphotypes are organized in Appendix S5.

### 3.2 Ornamentation variation within species

#### 3.2.1 Our samples

Eight species were chosen for testing the variation of pollen ornamentation among different specimens within species. Seven species (87.5%), present variability of the pollen surface ornamentation among different specimens (Fig. 4). For example, although three specimens of *Chusquea tessellata* were all collected from a tropical moist forest vegetation type in Colombia, their morphotypes are quite different, including *Avena*-type, *Triticum*-type, and *Hordeum*-type (Figs. 4B1–4B3). This is the first time that within-species variation in the pollen exine sculpture is reported for the Poaceae.

#### 3.2.2 Literature study

For five species, multiple plant specimens collected from different locations were found in different publications (Appendix S7). We found that pollen surface ornamentation varied in two of these five species (Table 3). The *Stipa*-type and the *Hordeum*-type were found within *Setaria verticillata* (L.) P. Beauv. (Morgado et al., 2015; Ullah et al., 2021). Within-species variation was also found in domesticated crops such as *Zea mays*, with the *Hordeum*-type and *Stipa*-type both observed in this species (Watson & Bell, 1975; Morgado et al., 2015). Moreover, the pollen ornamentation of two of our South American species, *Streptochoeta spicata* and *Olyra micrantha* Kunth, was earlier reported (Page, 1978; Mander & Punyasena, 2015; Dórea et al., 2017), and additional morphotypes for each species were identified. Specifically, the *Hordeum*-type and *Setaria*-type were found in *S. spicata* (Dórea et al., 2017) and *O. micrantha* (Page, 1978).

### 3.3 Morphotypes with rugulate structure

An overarching rugulate surface structure has been reported in the literature for grass pollen (i.e., Souza et al., 2021), which we found in several morphotypes. In these morphotypes, the pollen sculpture elements are fused and form irregularly arranged, winding shapes that comprise the entire pollen surface (Fig. 5). For example, the normal “*Avena*-type” has larger irregular, polygonal or elongate areolae studded with several 1–10 spinules (Köhler & Lange, 1979), similar to *Bothriochloa pertusa* (L.) A. Camus (Fig. 3B). For the “*Avena*-type” with rugulate structure, the adjacent areolae rise and fall one after another, showing a corrugated ornamentation of the entire pollen as observed in *Sporobolus multi-ramosus* Longhi-Wagner & Boechat (Guimarães et al., 2018). Similar rugulate structures were observed in the *Hordeum*-type, *Stipa*-type, *Setaria*-type, with their corresponding rugulate ornamentation found from *Atractantha*

**Table 2** The description of five new pollen surface morphotypes from existing publications.

Morphotypes	Overall	Areolae	Spinules/Scabrate	Reticulum	References
<i>Anomochloa</i> -type	Single detached spinules or areolae with 1–4 spinules	Larger irregular polygonal or elongated areolae	1–4 studded on the areolae	-	<i>Anomochloa marantoidea</i> Fig. 1E Dórea et al. (2017)
<i>Diandrolyra</i> -type	Mostly formed by long and tapering pointed spinule and few rounded scabrate	-	Dense single long and tapering pointed spinule; few rounded scabrate	-	<i>Diandrolyra pygmaea</i> Fig. 12K Dórea et al. (2017)
<i>Olyra bahiensis</i> -type	Few layers of overlapping areolae studded with 1–3 spinules	Dense irregular elongated, overlapping areolae	1–3 granules were studded on areolae	Scarcely	<i>Olyra bahiensis</i> Fig. 7E Dórea et al. (2017)
<i>Olyra juruana</i> -type	Undulations with a cauliflower-like surface structure, studded with single scabrate	-	Single rounded scabrate	-	<i>Olyra juruana</i> Fig. 13E Dórea et al. (2017)
<i>Sucrea</i> -type	Dense elongated striate, generally parallel, studded by sparse scabrate or spinules on the rugulate (element)	-	Sparse scabrate or with spinules studded on the rugulate (element) surface	-	<i>Sucrea sampaiana</i> Fig. 15H Dórea et al. (2017)

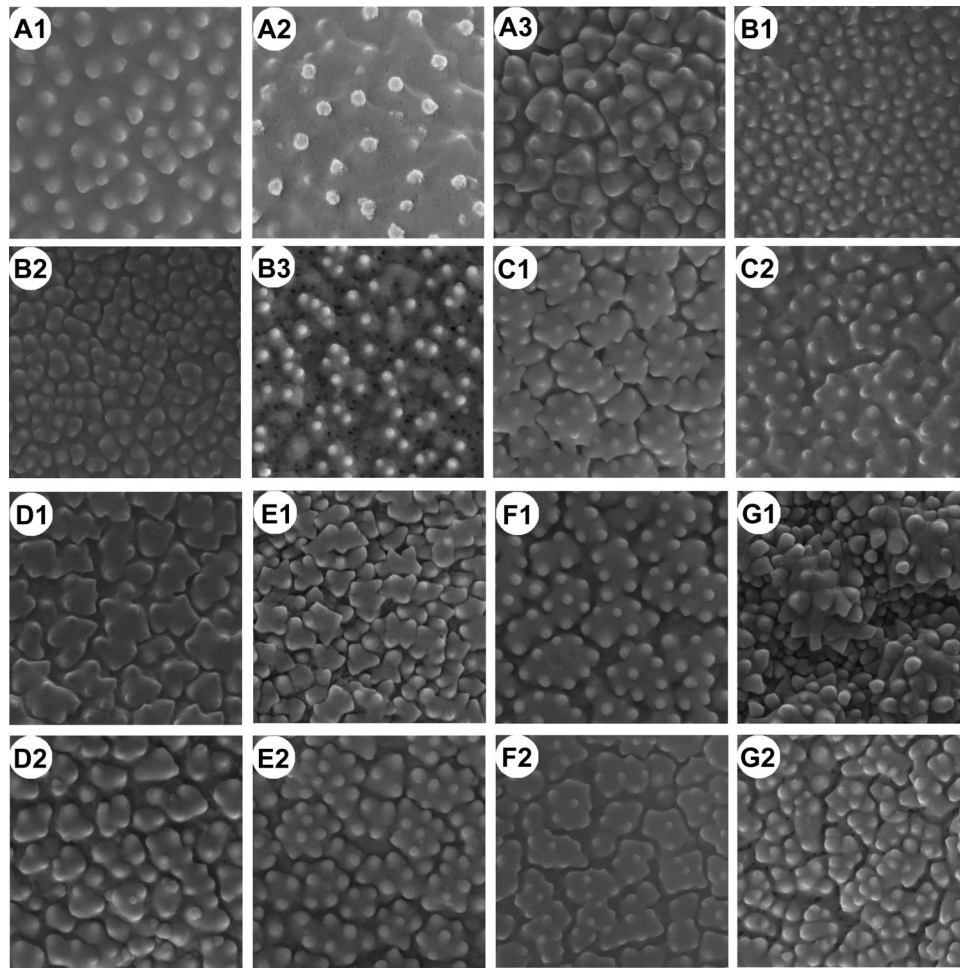


**Fig. 4.** Thumbnails showing the multitypes among specimens within species. A1–A3 are *Aristida recurvata* Kunth, three morphotypes of *Hordeum* (A1), *Stipa* (A2), and *Triticum* (A3) were identified, respectively. B1–B3 are *Chusquea tessellata*, with *Avena*-type (B1), *Triticum*-type (B2), and *Hordeum*-type (B3). C1–C2 are *Paspalum repens*, with *Avena*-type (C1), *Hordeum*-type (C2). D1, D2 are *Echinochloa colon* (L.) Link, with *Poa*-type (D1) and *Triticum*-type (D2). E1, E2 is *Poa annua*, with *Poa*-type (E1) and *Avena*-type (E2). F1, F2 is *Sporobolus indicus* (L.) R. Br., with *Avena*-type (F1) and *Setaria*-type (F2). G1, G2 are *Streptochaeta spicata*, with *Streptochaeta*-type (G1) and *Avena*-type (G2). Scale bar = 1  $\mu\text{m}$ .

**Table 3** Multitypes among specimens within species from existing publications.

Species	Morphotypes	References
<i>Setaria verticillata</i>	<i>Hordeum</i> -type	Plate5. 1 from Ullah et al. (2021)
	<i>Stipa</i> -type	Fig. 4. 42b from Morgado et al. (2015)
<i>Zea mays</i>	<i>Stipa</i> -type	Fig. 4. 45c from Morgado et al. (2015)
	<i>Hordeum</i> -type	Fig. 27. from Watson & Bell (1975)



**Fig. 5.** An example of *Dendrocalamus asper* showing the rugulate structure in grass pollen. Image credits: Priscilla Fernandes de Souza, Pardino, Brazil.

*falcata* McClure (Dórea et al., 2017), *Dendrocalamus asper* (Souza et al., 2021) and *Trichantheium polycomum* (Trin.) Zuloaga & Morrone (Guimarães et al., 2018), respectively. Here, we interpret them as common morphotypes but with a special rugulate structure (Table 4).

### 3.4 Overview of pollen surface ornamentation types in the Poaceae

By combining our samples and published SEM data, we constructed an updated database for grass pollen surface ornamentation, which includes 243 specimens from 223 species (Appendix S7), which were distributed in a wide variety of climates and environments. These samples represent 11 subfamilies across the grass phylogeny. A total of 15 morphotypes were identified, with nine of these characterized for the first time and added as new types, including the *Arthrostylidium*-type, *Anomochloa*-type, *Diandrolyra*-type, *Muhlenbergia*-type, *Olyra juruana*-type, *Olyra bahiensis*-type, *Poa*-type, *Streptochaeta*-type, and *Sucrea*-type. Nine of the 10 morphotypes that are present in our South American samples were found in the published literature. In general, the *Avena*-type, *Setaria*-type, *Hordeum*-type, *Stipa*-type, and *Triticum*-type are most common (Fig. 6).

### 3.5 Correlation between human-defined pollen morphotypes and quantitative analysis

Box plots were used to explore the relationship between the two quantified features (size and density) of pollen surface ornamentation and the human-defined morphotypes. Our results showed that each morphotype represents a unique morphological space of size or density, despite some variability that leads to an overlap between morphotypes. For *Stipa*-type, *Hordeum*-type, *Triticum*-type, *Avena*-type, and *Poa*-type, their log size and density both show a substantial increasing trend, and the log density value of *Poa*-type reached a peak. After the peak at the *Poa*-type, the value of log density of *Setaria*-type, *Arthrostylidium*-type, *Muhlenbergia*-type, and *Pariana*-type started to decrease. The *Streptochaeta*-type is the only one with both relatively large size and density (Figs. 7A, 7B). We conclude that human-defined morphotypes are well supported by computational analysis of the size and density features of sculptural elements.

### 3.6 Correlation between pollen ornamentation features and explanatory variables

Box plots, scatter plots, and regression were used to explore the correlation between pollen ornamentation features (size

**Table 4** Morphotypes with rugulate structure from existing publications.

Species	Morphotypes	References
<i>Sporobolus multiramosus</i>	<i>Avena</i> -type	Plate 1. 27–28 from Guimarães et al. (2018)
<i>Atractantha falcata</i>	<i>Hordeum</i> -type	Fig. 1G from Dórea et al. (2017)
<i>Dendrocalamus asper</i>	<i>Stipa</i> -type	Fig. 2C from Souza et al. (2021)
<i>Trichantheium polycomum</i>	<i>Setaria</i> -type	Plate 3. 3–5 from Guimarães et al. (2018)

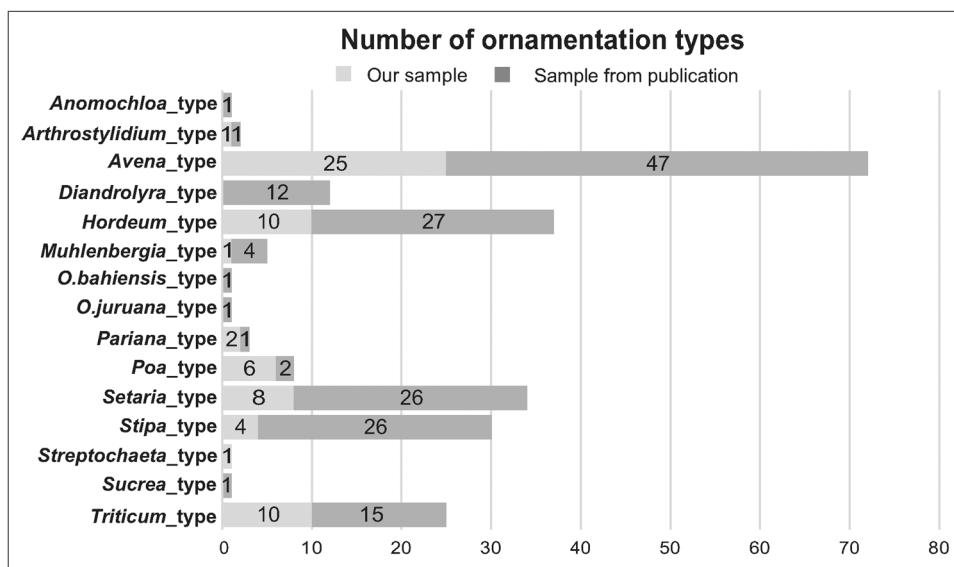


**Fig. 6.** Bar plot showing the frequency of each morphotype in terms of the number of plant specimens in our study. The light gray color is data from our sample, the dark gray color is data from published scanning electron microscope images from the literature.



and density) and six explanatory variables (Figs. 8, 9; Appendix S6). The distribution of log size and log density across each box plot of these six variables showed a substantial overlap with similar median values. Our results suggest that pollen ornamentation does not show a clear relationship with vegetation type, soil type, photosynthetic pathway, elevation, MAT, or TAP.

## 4 Discussion

### 4.1 Overview of our results

The main focus of our work was to explore the variation in pollen surface ornamentation and to determine if there is a correlation with their taxonomic position in the Poaceae. Scientists previously grouped grass pollen surface types into

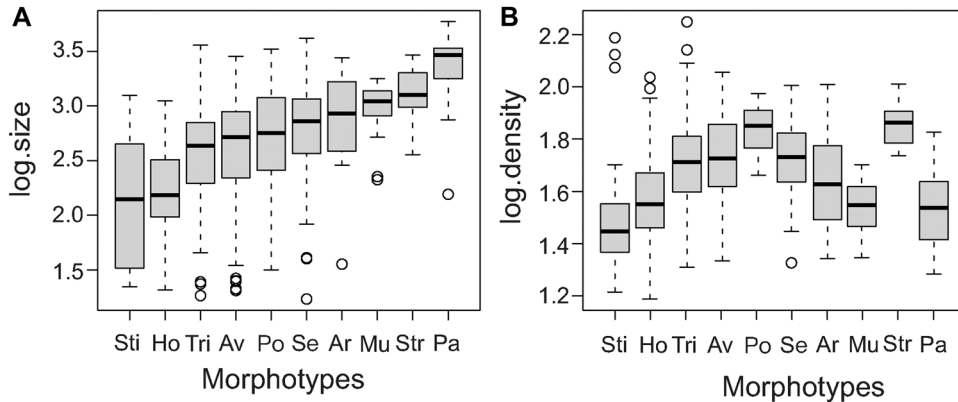


**Fig. 7.** Box plots of pollen surface morphotypes against (A) log size and (B) log density. The abbreviations on the x-axis represent left to right: *Stipa*-type, *Hordeum*-type, *Triticum*-type, *Avena*-type, *Poa*-type, *Setaria*-type, *Arthrostylidium*-type, *Muhlenbergia*-type, *Streptochoeta*, and *Pariana*-type.

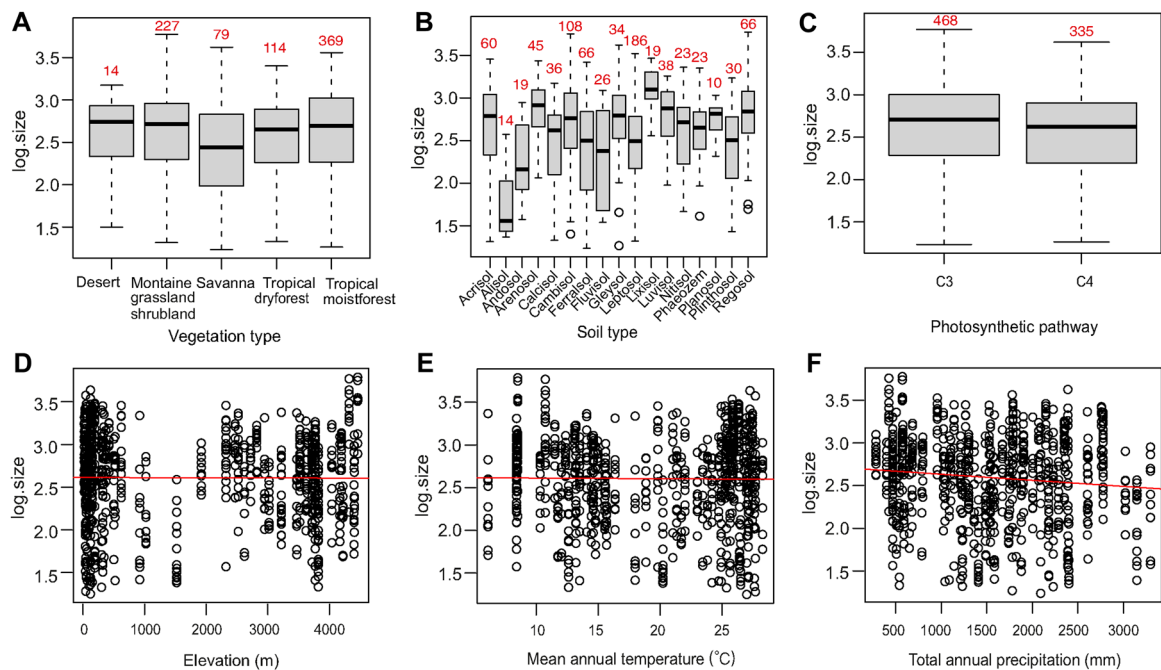


**Fig. 8.** Log size of Poaceae pollen ornamentation plotted against the six explanatory variables used in this study. **A–C.** Box plots of pollen ornamentation size against (A) vegetation type, (B) soil type, and (C) photosynthetic pathway. **D–F.** Scatter plots of pollen ornamentation size against (D) elevation, (E) mean annual temperature (°C), and (F) total annual precipitation (mm). The red number above the boxes represents the number of samples. The red line of the scatterplot represents a linear regression.

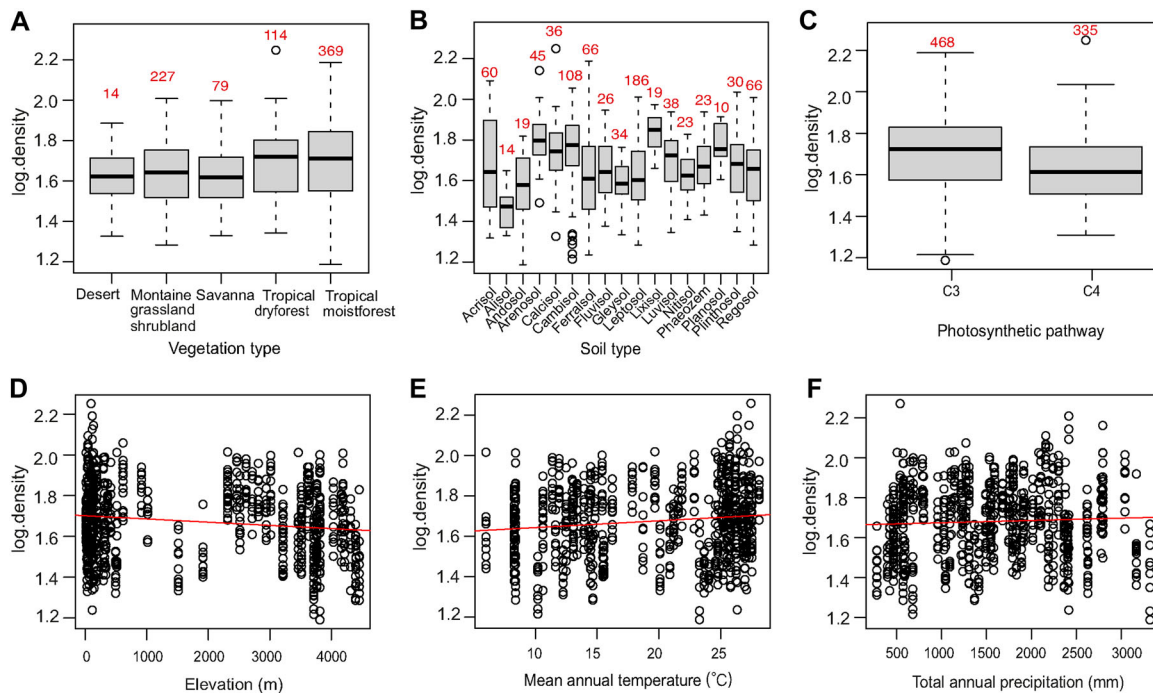


**Fig. 9.** Log density of Poaceae pollen ornamentation plotted against the six explanatory variables used in this study. **A–C,** Box plots of pollen ornamentation density against (A) vegetation type, (B) soil type, and (C) photosynthetic pathway. **D–F,** Scatter plots of pollen ornamentation density against (D) elevation, (E) mean annual temperature, and (F) total annual precipitation. The red number above the boxes represents the number of samples. The red line of the scatterplot represents a linear regression.

six morphotypes (e.g., Köhler & Lange, 1979; Mander & Punyasena, 2015). However, this number may not represent the entire pollen morphotype variation within the Poaceae. In addition, we question if morphotypes have taxonomic and paleoecological relevance beyond their original use with domesticated grasses. In our study, we aimed to address this problem through extensive sampling across northern South America and the use of data collected from other localities reported in the literature. We identified nine new and six known pollen surface morphotypes in total. These types are well supported by quantitative analysis of the size and density of sculptural elements of the pollen surface. We revealed that grass pollen surface ornamentation is diverse across the phylogeny.

#### 4.2 Is qualitative analysis useful and what does it tell us?

Until now, researchers found that Poaceae pollen surface ornamentation has a high degree of variability that can be classified into different morphological groups or morphotypes (Köhler & Lange, 1979; Mander & Punyasena, 2015). However, there is no assessment of the degree to which each morphotype can be supported by quantitative analyses of the surface ornamentation. In our study, we aimed to assess whether quantitative analysis supports these and other (new) pollen ornamentation morphotypes, when applied to extensive sampling.

Ten morphotypes were identified by the human eye from 68 samples collected from different environments in northern South America. Furthermore, after extracting two

features of the ornamentation (size and density) based on the SEM images, we found that each morphotype represents a unique morphological space of size or density, despite some variability which leads to overlap between morphotypes (Fig. 7). A trend that is consistent with the results observed by the human eye level, that is, different morphotypes are partially related, and partially different from each other. Therefore, we conclude that human-defined morphotypes are well supported by computational analysis of the size and density features of sculptural elements, and change following a sliding scale trend. We also evaluated the relevance of the quantitative characters of these ten morphotypes with several key explanatory variables, including vegetation type, soil composition, photosynthetic pathway, elevation, temperature, and precipitation. However, there is no clear relationship between them.

#### 4.3 Do morphotypes vary across the phylogenetic tree?

The Poaceae subfamilies are traditionally grouped into three early diverging monophyletic groups and two major clades (e.g., Linder, 1987; Grass Phylogeny Working Group I [GPWG] et al., 2001; Linder & Rudall, 2005; GPWG II, 2012; Soreng et al., 2022). Anomochloideae, Pharioideae, and Puelioideae form the early diverging monophyletic groups; Oryzoideae, Bambusoideae, and Pooideae form the BOP clade, and Aristidoideae, Panicoideae, Arundinoideae, Micraioideae, Danthonioideae, and Chloridoideae form the PACMAD clade (e.g., GPWG et al., 2001; Sánchez-Ken & Clark, 2010; Soreng et al., 2015).

We found that pollen surface morphotypes varied both at genus and species level, which is consistent with some earlier studies (e.g., Morgado et al., 2015; Dórea et al., 2017). Moreover, we found multimorphic exine sculpture patterns occurs among different specimen within species of grass (Figs. 4, 6). A few cases showed that dimorphic pollen exine structures were found within species in some subfamilies, such as *Cocos nucifera* L. from Arecaceae (Nair & Sharma, 1963), three *Linum* (*Linum grandiflorum* Desf., *Linum mucronatum* Bertol., and *Linum pubescens* Banks & Sol.) from Linaceae (Dulberger, 1981], *Dyerophytum africanum* (Lam.) Kuntze and *D. indicum* Kuntze (Plumbaginaceae) (Weber-El Ghobary, 1986). Such variation suggests that, based on surface ornamentation, more pollen morphotypes will appear if further examination of intra-specific and/or interspecific levels is carried out.

When linking pollen surface ornamentation to the dated phylogenetic tree, we notice that the amount of pollen morphotypes identified in our study correlates with the number of species in a subfamily (Fig. 10). The ancient subfamilies (Anomochlooideae, Pharodieae, Puelidideae) that are rooted in the early Cretaceous (101 Ma) (Huang et al., 2022), are low in species richness and have also limited morphological types. In contrast, morphotypes from PACMAD and BOP clades are much more diverse, which split from each other at 81.43 Ma and became hugely species-rich in the Miocene (<23 Ma; Stromberg, 2011; Gallaher et al., 2022; Huang et al., 2022). From

this, we conclude that grass pollen morphology is diverse across the phylogeny.

**4.3.1 Four common morphotypes throughout the grass phylogeny**

We noted that there are four common morphotypes, which already were identified in the 1970s (Köhler & Lange, 1979), including *Avena*-type, *Hordeum*-type, *Setaria*-type, and *Triticum*-type. These morphotypes are found in the ancient subfamilies (Anomochlooideae, Pharodieae, Puelidideae) and the PACMAD and Bambusoideae–Oryzoideae–Pooideae (BOP) clades. These subfamilies and their clades are distributed across elevations and in different climates, soils, and environmental systems (Gibson, 2009; Blair et al., 2014; Linder et al., 2018), which also explains why the morphotypes, which are delimited by small variations in the size and density of the sculptural elements, are not obviously correlated with the tested explanatory variables (vegetation type, soil composition, photosynthetic pathway, elevation, and climate data) (Figs. 8–10).

**4.3.2 Unique morphotypes point at taxonomic position**

According to the current estimate, six morphotypes are found with unique taxonomic positions. The *Anomochloa*-type and *Streptochaeta*-type were only found in the ancient Anomochlooideae subfamily. In Bambusoideae, the *Diandrolyra*-type, *Olyra bahiensis*-type, *Olyra juruana*-type, and *Sucrea*-type were also unique (Fig. 10). It is worth emphasizing that a

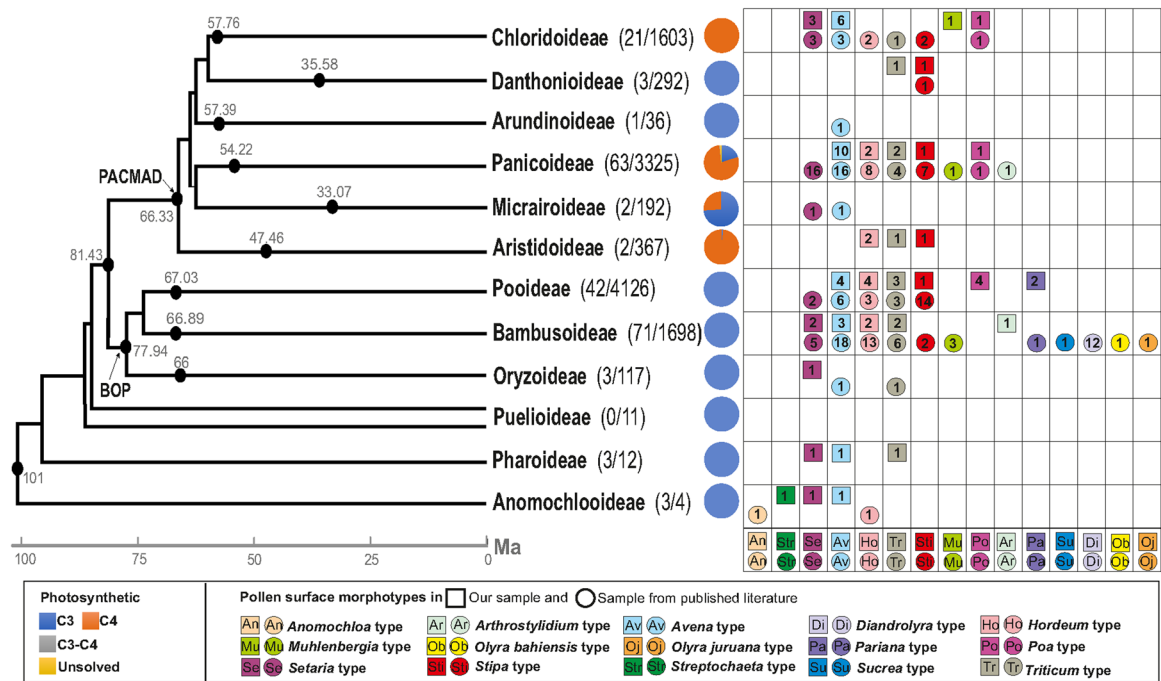


**Fig. 10.** Pollen surface ornamentation shows diversity across the Poaceae phylogeny. A Poaceae time tree estimated from molecular data and calibrated by fossil records, redrawn from Huang et al. (2022). BOP, Bambusoideae–Oryzoideae–Pooideae; PACMAD, Panicoideae–Arundinoideae–Chloridoideae–Micrairoideae–Aristidoideae–Danthonioideae. Numbers in brackets represent the species richness (species number with scanning electron microscope image/number of total species) among the subfamilies (Soreng et al., 2022). The pie chart represents the proportion of photosynthetic pathways of species in each subfamily (Appendix S2). The different colors and the number of symbols (square or circle) in the grid show the distribution of the 15-grass pollen morphotypes identified by each specimen in each subfamily.

detailed sample analysis that incorporates fossils to estimate the changes in these morphotypes through time holds great promise. Such studies could indicate when the different grass pollen morphotypes evolved, and such knowledge could be used to measure changes in the diversity and composition of grasses through geological time.

As we are working with extant taxa, we cannot be sure when the morphotypes emerged. In principle, it is possible that they all were generated in the Cretaceous, but it is equally possible that they appeared in the Quaternary. The emergence of the variation in morphotypes could be tested by studying the fossil record through further palynological analysis. Some of our morphotypes are unique and potentially can be used to identify subfamilies. For subfamilies with a large variation in morphotypes, it will be difficult to use pollen morphotypes as an identifier.

In summary, we reported the current estimate for grass pollen surface ornamentation morphotype variation throughout their phylogeny. The pollen ornamentation morphotypes can be supported by quantitative analysis, and the degree of variation is consistent with the species richness of the subfamily. However, we are still limited as many Poaceae species are underexplored from a palynological point of view—the known pollen surface ornamentation of Poaceae is only 1.9% (223/11783) (Soreng et al., 2022) of the total number of species. More work will be needed, on both extant and fossil grass pollen, and it is likely that many more morphotypes will be found in the future. We especially encourage scientists to focus on the surface ornamentation of fossil pollen to assess Poaceae surface variation types across the geological timescale. Further study is also needed to define if, and when, these morphotypes first occurred in the fossil record, and if the emergence of a large amount of diversity of pollen morphotypes occurred in the Cretaceous, when the Poaceae first evolved. Or if perhaps it was much later, in the Miocene, during the diversification of the grasses and the rise of grassland biomes (Palazzesi et al., 2022).

#### 4.4 Implications for the wider research community

Linking the grass pollen morphotypes to databases detailing biogeographic, climatic, (paleo)botanical, and (paleo)ecological studies is already possible, permitting the application of tools developed for spatial and time ecology. Furthermore, paleoecologists would benefit from incorporating morphotypes to fossil grass pollen data, to elucidate the changes of these morphotypes through time. In the field of allergy and immunology studies, grass pollen is also utilized as a potential tool for diagnosing and/or preventing seasonal allergies. (i.e., Vinckier & Smets, 2001; Yasniuk et al., 2020) Our results may also be relevant in the context of allergy studies, as grass pollen morphology could play a role in allergic diseases.

## 5 Conclusion

We have examined the pollen from extant plant samples across northern South America to construct a reference framework for Poaceae pollen based on surface orna-

mentation. The human-eye-level identified pollen morphotypes could be well supported by the extraction of two quantitative features (sculptural elements size and density) using computational analysis. The influence of vegetation type, soil type, photosynthetic pathway, elevation, and climate data does not seem to control the expression of a morphotype. The morphological richness of pollen surface ornamentation correlates with species richness at the subfamily level. Here, we represent an updated database of pollen surface ornamentation morphotypes of Poaceae, nevertheless, there is still some limitation as many Poaceae species remain unexplored (98.1% of the total amount of species). We encourage more scientists to focus on the combination of high-resolution imaging of extant and fossil grass pollen surface ornamentation and computational image analysis to elucidate the (paleo-)ecology of grasslands. To validate if our finding based on modern material holds through evolutionary time next steps for this research would be to seek to identify the different morphotypes within pollen extracted from the fossil record. The (in)dependence of morphotype development from species evolution could provide valuable new insights into the mechanisms behind diversification.

## Acknowledgements

We thank Marnel Scherrenberg (Naturalis Biodiversity Center) for specimen collection, especially during the COVID-19 pandemic; Henry Hooghiemstra (University of Amsterdam) for pollen collection from anthers; Annelise Philip (University of Amsterdam) for processing pollen samples; Bertie Joan van Heuven (Naturalis Biodiversity Center) for sharing the constructive experience and suggestion for processing pollen grains for scanning electron microscope (SEM) experiment; Yan Fang (Nanjing Institute of Geology and Paleontology, Chinese Academy of Sciences, Nanjing, China) and Edwin Scholl (Electron Microscopy Center Amsterdam, Amsterdam UMC) for technical assistance in the collection of the SEM images. We thank Surangi W. Punyasena and another anonymous reviewer for their insightful comments on the manuscript. C.W. acknowledges the China Scholarship Council (CSC) grant and bursary funding from IBED, University of Amsterdam. P.E.J. acknowledges funding from the Deutsche Forschungsgemeinschaft (DFG, German Research Foundation) project number 443701866. SEM imaging was financially supported by the grants XDB26000000 and 41877437 (Nanjing Institute of Geology and Paleontology, Chinese Academy of Sciences, Nanjing, China).

## Authors Contributions

Caixia Wei: Conceptualization, data curation, formal analysis, investigation, methodology, software, project administration, visualization, validation, writing—original draft and writing—review and editing; Phillip E. Jardine: Conceptualization, methodology, software, supervision, visualizations, writing—review and editing; L.Mao: Methodology; funding

acquisition, writing—review and editing; Luke Mander: Conceptualization, methodology, validation, writing—review and editing; Mao Li: Methodology, software, visualization, writing—review and editing; William D. Gosling: Conceptualization, writing—review and editing; Carina Hoorn: Conceptualization, investigation, and validation, project administration, supervision, writing—review and editing. All authors gave final approval for publication and agreed to be held accountable for the work performed therein.

## Conflict of Interest

Caixia Wei, Phillip E. Jardine, Limi Mao, Luke Mander, Mao Li, William D. Gosling, and Carina Hoorn declare no conflict of interest.

## References

- Anar M, Ahmad M, Zafar S, Elnaggar AY, Zafar M, Sultana S, Tariq A, Anjum F, Hussein EE, Kiliç Ö, Ozdemir FA. 2022. Palynomorphological diversity of Asteraceous and Poaceus allergenic plant using microscopic techniques in lesser Himalaya-Pakistan. *Microscopy Research and Technique* 85: 2061–2075.
- Andersen TS, Bertelsen F. 1972. Scanning electron microscope studies of pollen of cereals and other grasses. *Grana* 12: 79–86.
- Beug HJ. 2004. Leitfaden der pollenbestimmung für Mitteleuropa und angrenzende Gebiete. *Verlag Friedrich Pfeil* 21: 542.
- Blair J, Nippert J, Briggs J. 2014. Grassland ecology 14. *Ecology and the Environment* 389: 389–423.
- Bush MB. 2002. On the interpretation of fossil Poaceae pollen in the lowland humid neotropics. *Palaeogeography, Palaeoclimatology, Palaeoecology* 177: 5–17.
- Christin P-A, Osborne CP, Chatelet DS, Columbus JT, Besnard G, Hodkinson TR, Garrison LM, Vorontsova MS, Edwards EJ. 2013. Anatomical enablers and the evolution of C<sub>4</sub> photosynthesis in grasses. *Proceedings of the National Academy of Sciences of the United States of America* 110: 1381–1386.
- Chaturvedi M, Datta K, Nair PKK. 1998. Pollen morphology of *Oryza* (Poaceae). *Grana* 37: 79–86.
- Dórea MC, Santos DWJ, Oliveira RP, Funch LS, Santos FAR. 2018. Reproductive traits related to anemophily and insect visitors in two species of Poaceae from the Brazilian Atlantic rainforest. *Brazilian Journal of Botany* 41: 425–434.
- Dórea MDC, de Oliveira RP, Banks H, dos Santos F, De AR. 2017. Sculptural elements on the ectexine surface of Poaceae pollen from Neotropical forests: Patterns and implications for taxonomic and evolutionary studies in this family. *Botanical Journal of the Linnean Society* 185: 542–571.
- Dulberger R. 1981. Dimorphic exine sculpturing in three distylous species of *Linum* (Linaceae). *Plant Systematics and Evolution* 139: 113–119.
- Ferguson IK, Verdcourt B, Poole MM. 1977. Pollen morphology in the genera *Merremia* and *Operculina* (Convolvulaceae) and its taxonomic significance. *Kew Bulletin* 31: 763–773.
- Gallaher TJ, Peterson PM, Soreng RJ, Zuloaga FO, Li DZ, Clark LG, Tyrrell CD, Welker CA, Kellogg EA, Teisher JK. 2022. Grasses through space and time: An overview of the biogeographical and macroevolutionary history of Poaceae. *Journal of Systematics and Evolution* 60: 522–569.
- Gibson DJ. 2009. *Grasses and grassland ecology*. UK: Oxford University Press.
- Grass Phylogeny Working Group (GPWG) II. 2012. New grass phylogeny resolves deep evolutionary relationships and discovers C<sub>4</sub> origins. *New Phytologist* 193: 304–312.
- Grass Phylogeny Working Group (GPWG), Barker GP, NP L, Clark JI, Davis MR, Duvall MR, Guala GF, Hsiao C, Kellogg EA, Linder HP, Mason-Gamer RJ, Mathews SY. 2001. *Annals of the Missouri Botanical Garden* 88: 373–457. <https://doi.org/10.2307/3298585>
- Guimarães JTF, Carreira LMM, Alves R, Souza Filho PWM, Giannini TC, Macambira HJ, Silva EF, Dias ACR, Silva CB, Araújo Romeiro L, Rodrigues TM. 2018. Pollen morphology of the Poaceae: Implications of the palynological and paleoecological records of the southeastern Amazon in Brazil. *Palynology* 42: 311–323.
- Halbritter H, Ulrich S, Grímsson F, Weber M, Zetter R, Hesse M, Buchner R, Svojtka M, Frosch-Radivo A. 2018. *Illustrated pollen terminology*. Vienna, Austria: Springer.
- Huang W, Zhang L, Columbus JT, Hu Y, Zhao Y, Tang L, Guo Z, Chen W, McKain M, Bartlett M, Huang CH. 2022. A well-supported nuclear phylogeny of Poaceae and implications for the evolution of C<sub>4</sub> photosynthesis. *Molecular Plant* 15: 755–777.
- Ibrahim DG, Burke T, Ripley BS, Osborne CP. 2009. A molecular phylogeny of the genus *Alloteropsis* (Panicoideae, Poaceae) suggests an evolutionary reversion from C<sub>4</sub> to C<sub>3</sub> photosynthesis. *Annals of Botany* 103: 127–136.
- Kadereit G, Bohley K, Lauterbach M, Tefarikis DT, Kadereit JW. 2017. C<sub>3</sub>–C<sub>4</sub> intermediates may be of hybrid origin—A reminder. *New Phytologist* 215: 70–76.
- Köhler E, Lange E. 1979. A contribution to distinguishing cereal from wild grass pollen grains by LM and SEM. *Grana* 18: 133–140.
- Lee G-A, Davis AM, Smith DG, McAndrews JH. 2004. Identifying fossil wild rice (*Zizania*) pollen from Cootes Paradise, Ontario: A new approach using scanning electron microscopy. *Journal of Archaeological Science* 31: 411–421.
- Linder HP. 1987. The evolutionary history of the Poales/Restionales: A hypothesis. *Kew Bulletin* 42: 297–318.
- Linder HP, Lehmann CER, Archibald S, Osborne CP, Richardson DM. 2018. Global grass (Poaceae) success underpinned by traits facilitating colonization, persistence and habitat transformation. *Biological Reviews* 93: 1125–1144.
- Linder HP, Rudall PJ. 2005. Evolutionary history of Poales. *Annual Review of Ecology, Evolution, and Systematics* 36: 107–124.
- López-Merino L, Leroy SAG, Haldorsen S, Heun M, Reynolds A. 2015. Can *Triticum urartu* (Poaceae) be identified by pollen analysis? Implications for detecting the ancestor of the extinct two-grained einkorn-like wheat. *Botanical Journal of the Linnean Society* 177: 278–289.
- Lovisolo MR, Galati BG. 2012. Diversidad de orbículas en Poaceae. *Boletín de la Sociedad Argentina de Botánica* 47: 87–96.
- Mander L, Li M, Mio W, Fowlkes CC, Punyasena SW. 2013. Classification of grass pollen through the quantitative analysis of surface ornamentation and texture. *Proceedings of the Royal Society B: Biological Sciences* 280: 20131905.
- Mander L, Punyasena SW. 2015. Grass pollen surface ornamentation: A review of morphotypes and taxonomic utility. *Journal of Micropalaeontology* 35: 121–124.
- Mercuri AM, Clò E, Florenzano A. 2022. Multiporate pollen of Poaceae as bioindicator of environmental stress: First archaeobotanical evidence from the early–middle Holocene site of Takarkori in the central Sahara. *Quaternary* 5: 41.

- Moore NA, Camac JS, Morgan JW. 2019. Effects of drought and fire on resprouting capacity of 52 temperate Australian perennial native grasses. *New Phytologist* 221: 1424–1433.
- Morgado LN, Gonçalves-Esteves V, Resendes R, Ventura MAM. 2015. Pollen morphology of Poaceae (Poales) in the Azores, Portugal. *Grana* 54: 282–293.
- Nair PKK, Sharma M. 1963. Pollen grains of *Cocos Nucifera* Linn. *Grana* 4: 373–379.
- Needham I, Vorontsova MS, Banks H, Rudall PJ. 2015. Pollen of Malagasy grasses as a potential tool for interpreting grassland palaeohistory. *Grana* 54: 247–262.
- Noor MJ, Ahmad M. 2021. Scanning electron imaging of mellitophilous and allergenic pollen grain of arid and northern irrigated agroecological zones of Pakistan. *Microscopy Research and Technique* 84: 1834–1861.
- Osborne CP, Salomaa A, Kluyver TA, Visser V, Kellogg EA, Morrone O, Vorontsova MS, Clayton WD, Simpson DA. 2014. A global database of C4 photosynthesis in grasses. *New Phytologist* 2014: 441–446.
- Page JS. 1978. A scanning electron microscope survey of grass pollen. *Kew Bulletin* 32: 313–319.
- Palazzesi L, Hidalgo O, Barreda VD, Forest F, Höhna S. 2022. The rise of grasslands is linked to atmospheric CO<sub>2</sub> decline in the late Palaeogene. *Nature Communications*, 13(1): 293.
- Poinar GJ, Alderman S, Wunderlich J. 2015. One hundred million year old ergot: Psychotropic compounds in the Cretaceous. *Palaeodiversity* 8: 13–19.
- Prasad V, Strömberg CAE, Alimohammadian H, Sahni A. 2005. Paleontology: Dinosaur coprolites and the early evolution of grasses and grazers. *Science* 310: 1177–1180.
- Punt W, Hoen PP, Blackmore S, Nilsson S, Le Thomas A. 2007. Glossary of pollen and spore terminology. *Review of Palaeobotany and Palynology* 143: 1–81.
- R Core Team. 2021. R: A language and environment for statistical computing. Foundation for Statistical Computing, Vienna.
- Renvoize SA. 1981. The sub-family Arundinoideae and its position in relation to a general classification of the Gramineae. *Kew Bulletin* 36: 85–102.
- Renvoize SA. 1986. A survey of leaf-blade anatomy in grasses VIII. *Arundinoideae*. *Kew Bulletin* 37: 323–338.
- Romero IC, Kong S, Fowlkes CC, Jaramillo C, Urban MA, Obok-Ikuenobe F, D'Apolito C, Punyasena SW. 2020. Improving the taxonomy of fossil pollen using convolutional neural networks and superresolution microscopy. *Proceedings of the National Academy of Sciences United States of America* 117: 28496–28505.
- Ruggiero F, Bedini G. 2018. Systematic and morphologic survey of orbicules in allergenic angiosperms. *Aerobiologia* 34: 405–422.
- Sánchez-Ken JG, Clark LG. 2010. Phylogeny and a new tribal classification of the Panicoideae s1 (Poaceae) based on plastid and nuclear sequence data and structural data. *American Journal of Botany* 97(10): 1732–1748.
- Salgado-Labouriau ML, Rinaldi M. 1990. Palynology of Gramineae of the Venezuelan mountains. *Grana* 29: 119–128.
- Soreng RJ, Peterson PM, Romaschenko K, Davidse G, Zuloaga FO, Judziewicz EJ, Filgueiras TS, Davis JI, Morrone O. 2015. A worldwide phylogenetic classification of the Poaceae (Gramineae). *Journal of Systematics and Evolution* 53: 117–137.
- Soreng RJ, Peterson PM, Zuloaga FO, Romaschenko K, Clark LG, Teisher JK, Gillespie LJ, Barberá P, Welker CA, Kellogg EA, Li DZ. 2022. A worldwide phylogenetic classification of the Poaceae (Gramineae) III: An update. *Journal of Systematics and Evolution* 60: 476–521.
- Souza PFde, Santos CMRdos, Ree J, Guerra MP, Pescador R. 2021. Flowering and morphological characterization of *Dendrocalamus asper* androecium and pollen grains. *Grana* 60: 20–34.
- Stromberg CAE. 2011. Evolution of grasses and grassland ecosystems. *Annual Review of Earth and Planetary Sciences* 39: 517–544.
- Toledo JAM, Rossi ML, de Andrade Bressan E, Shirasuna RT, Martinelli AP, Oliveira GCX. 2022. Floral characteristics, pollen morphology, and viability of sugarcane hybrids (*Saccharum officinarum*) and the neotropical wild relative, *S. villosum*. *Flora* 294: 152118.
- Ullah I, Ahmad M, Jabeen A, Yusuf MO, Arfan M, Kilic O, Bagci E, Zafar M, Sultana S, Khan S, Usma A. 2021. Palynomorphological characterization of selected allergenic taxa of family Poaceae from Islamabad-Pakistan using microscopic techniques. *Microscopy Research and Technique* 84: 2544–2558.
- Vinckier S, Smets E. 2001. The potential role of orbicules as a vector of allergens. *Allergy* 56: 1129–1136.
- Vizez N, Nadaï P, Choël M, Farah J, Hamzé M, Sénéchal H, Pauwels M, Frérot H, Thibaudon M, Poncet P. 2021. Biochemical composition of *Phleum pratense* pollen grains: A review. *Molecular Immunology* 136: 98–109.
- Watson L, Bell EM. 1975. A surface-structural survey of some taxonomically diverse grass pollens. *Australian Journal of Botany* 23: 981–990.
- Weber-El Ghobary MO. 1986. Dimorphic exine sculpturing in two distylous species of *Dyerophytum* (Plumbaginaceae). *Plant Systematics and Evolution* 152: 267–276.
- Wei C, Jardine PE, Gosling WD, Hoorn C. 2023. Is Poaceae pollen size a useful proxy in palaeoecological studies? New insights from a Poaceae pollen morphological study in the Amazon. *Review of Palaeobotany and Palynology* 308: 104790.
- Wills KE, Whalley RDB, Bruhl JJ. 2000. Systematic studies in Paniceae (Poaceae): *Homopholis* and *Whalleya* gen. et sp. nov. *Australian Systematic Botany* 13: 437–468.
- White RP, Murray S, Rohweder M, Prince SD, Thompson KM. 2000. *Grassland ecosystems*. Washington, DC: World Resources Institute. 81.
- Wu Y, You HL, Li XQ. 2018. Dinosaur-associated Poaceae epidermis and phytoliths from the Early Cretaceous of China. *National Science Review* 5: 721–727.
- Yasniuk MV, Kaminska OA, Rodinkova V. 2020. Grass pollen morphology investigation as a basis for monitoring of allergenic biological particles in an automatic mode. *Reports of Morphology* 26: 32–38.

## Supplementary Material

The following supplementary material is available online for this article at <http://onlinelibrary.wiley.com/doi/10.1111/jse.13021/supinfo>:

**Appendix S1.** Sample information for the herbarium specimens sampled for this study.

**Appendix S2.** Quantifying pollen surface ornamentation information for the herbarium specimens sampled for this study.

**Appendix S3.** A global database of C<sub>3</sub>/C<sub>4</sub> photosynthesis in grasses.

**Appendix S4.** Scanning electron microscopy images for two *Oryza* species.

**Appendix S5.** Descriptions of 15 morphotypes found in this study.

**Appendix S6.** Scatter plots for correlation between pollen ornamentation features and explanatory variables.

**Appendix S7.** Database of grass morphotypes based on our sample and published scanning electron microscope images.